

EUROPEAN ORGANIZATION FOR NUCLEAR RESEARCH (CERN)



CERN-PH-EP-2012-214

LHCb-PAPER-2012-014

September 20, 2012

Measurement of the $B_s^0 \rightarrow J/\psi \bar{K}^{*0}$ branching fraction and angular amplitudes

The LHCb collaboration[†]

Abstract

A sample of 114 ± 11 $B_s^0 \rightarrow J/\psi K^- \pi^+$ signal events obtained with 0.37 fb^{-1} of pp collisions at $\sqrt{s} = 7 \text{ TeV}$ collected by the LHCb experiment is used to measure the branching fraction and polarization amplitudes of the $B_s^0 \rightarrow J/\psi \bar{K}^{*0}$ decay, with $\bar{K}^{*0} \rightarrow K^- \pi^+$. The $K^- \pi^+$ mass spectrum of the candidates in the B_s^0 peak is dominated by the \bar{K}^{*0} contribution. Subtracting the non-resonant $K^- \pi^+$ component, the branching fraction of $B_s^0 \rightarrow J/\psi \bar{K}^{*0}$ is $(4.4^{+0.5}_{-0.4} \pm 0.8) \times 10^{-5}$, where the first uncertainty is statistical and the second is systematic. A fit to the angular distribution of the decay products yields the K^{*0} polarization fractions $f_L = 0.50 \pm 0.08 \pm 0.02$ and $f_{||} = 0.19^{+0.10}_{-0.08} \pm 0.02$.

Submitted to Physical Review D (R)

[†]Authors are listed on the following pages.

LHCb collaboration

R. Aaij³⁸, C. Abellan Beteta^{33,n}, A. Adametz¹¹, B. Adeua³⁴, M. Adinolfi⁴³, C. Adrover⁶, A. Affolder⁴⁹, Z. Ajaltouni⁵, J. Albrecht³⁵, F. Alessio³⁵, M. Alexander⁴⁸, S. Ali³⁸, G. Alkhazov²⁷, P. Alvarez Cartelle³⁴, A.A. Alves Jr²², S. Amato², Y. Amhis³⁶, J. Anderson³⁷, R.B. Appleby⁵¹, O. Aquines Gutierrez¹⁰, F. Archilli^{18,35}, A. Artamonov³², M. Artuso^{53,35}, E. Aslanides⁶, G. Auriemma^{22,m}, S. Bachmann¹¹, J.J. Back⁴⁵, V. Balagura^{28,35}, W. Baldini¹⁶, R.J. Barlow⁵¹, C. Barschel³⁵, S. Barsuk⁷, W. Barter⁴⁴, A. Bates⁴⁸, C. Bauer¹⁰, Th. Bauer³⁸, A. Bay³⁶, J. Beddow⁴⁸, I. Bediaga¹, S. Belogurov²⁸, K. Belous³², I. Belyaev²⁸, E. Ben-Haim⁸, M. Benayoun⁸, G. Bencivenni¹⁸, S. Benson⁴⁷, J. Benton⁴³, R. Bernet³⁷, M.-O. Bettler¹⁷, M. van Beuzekom³⁸, A. Bien¹¹, S. Bifani¹², T. Bird⁵¹, A. Bizzeti^{17,h}, P.M. Bjørnstad⁵¹, T. Blake³⁵, F. Blanc³⁶, C. Blanks⁵⁰, J. Blouw¹¹, S. Blusk⁵³, A. Bobrov³¹, V. Bocci²², A. Bondar³¹, N. Bondar²⁷, W. Bonivento¹⁵, S. Borghi^{48,51}, A. Borgia⁵³, T.J.V. Bowcock⁴⁹, C. Bozzi¹⁶, T. Brambach⁹, J. van den Brand³⁹, J. Bressieux³⁶, D. Brett⁵¹, M. Britsch¹⁰, T. Britton⁵³, N.H. Brook⁴³, H. Brown⁴⁹, A. Büchler-Germann³⁷, I. Burducea²⁶, A. Bursche³⁷, J. Buytaert³⁵, S. Cadeddu¹⁵, O. Callot⁷, M. Calvi^{20,j}, M. Calvo Gomez^{33,n}, A. Camboni³³, P. Campana^{18,35}, A. Carbone¹⁴, G. Carboni^{21,k}, R. Cardinale^{19,i,35}, A. Cardini¹⁵, L. Carson⁵⁰, K. Carvalho Akiba², G. Casse⁴⁹, M. Cattaneo³⁵, Ch. Cauet⁹, M. Charles⁵², Ph. Charpentier³⁵, P. Chen^{3,36}, N. Chiapolini³⁷, M. Chrzaszcz²³, K. Ciba³⁵, X. Cid Vidal³⁴, G. Ciezarek⁵⁰, P.E.L. Clarke⁴⁷, M. Clemencic³⁵, H.V. Cliff⁴⁴, J. Closier³⁵, C. Coca²⁶, V. Coco³⁸, J. Cogan⁶, E. Cogneras⁵, P. Collins³⁵, A. Comerma-Montells³³, A. Contu⁵², A. Cook⁴³, M. Coombes⁴³, G. Corti³⁵, B. Couturier³⁵, G.A. Cowan³⁶, D. Craik⁴⁵, R. Currie⁴⁷, C. D'Ambrosio³⁵, P. David⁸, P.N.Y. David³⁸, I. De Bonis⁴, K. De Bruyn³⁸, S. De Capua^{21,k}, M. De Cian³⁷, J.M. De Miranda¹, L. De Paula², P. De Simone¹⁸, D. Decamp⁴, M. Deckenhoff⁹, H. Degaudentzi^{36,35}, L. Del Buono⁸, C. Deplano¹⁵, D. Derkach^{14,35}, O. Deschamps⁵, F. Dettori³⁹, J. Dickens⁴⁴, H. Dijkstra³⁵, P. Diniz Batista¹, F. Domingo Bonal^{33,n}, S. Donleavy⁴⁹, F. Dordei¹¹, A. Dosil Suárez³⁴, D. Dossett⁴⁵, A. Dovbnya⁴⁰, F. Dupertuis³⁶, R. Dzhelyadin³², A. Dziurda²³, A. Dzyuba²⁷, S. Easo⁴⁶, U. Egede⁵⁰, V. Egorychev²⁸, S. Eidelman³¹, D. van Eijk³⁸, F. Eisele¹¹, S. Eisenhardt⁴⁷, R. Ekelhof⁹, L. Eklund⁴⁸, I. El Rifai⁵, Ch. Elsasser³⁷, D. Elsby⁴², D. Esperante Pereira³⁴, A. Falabella^{16,e,14}, C. Färber¹¹, G. Fardell⁴⁷, C. Farinelli³⁸, S. Farry¹², V. Fave³⁶, V. Fernandez Albor³⁴, F. Ferreira Rodrigues¹, M. Ferro-Luzzi³⁵, S. Filippov³⁰, C. Fitzpatrick⁴⁷, M. Fontana¹⁰, F. Fontanelli^{19,i}, R. Forty³⁵, O. Francisco², M. Frank³⁵, C. Frei³⁵, M. Frosini^{17,f}, S. Furcas²⁰, A. Gallas Torreira³⁴, D. Galli^{14,c}, M. Gandelman², P. Gandini⁵², Y. Gao³, J-C. Garnier³⁵, J. Garofoli⁵³, J. Garra Tico⁴⁴, L. Garrido³³, D. Gascon³³, C. Gaspar³⁵, R. Gauld⁵², N. Gauvin³⁶, E. Gersabeck¹¹, M. Gersabeck³⁵, T. Gershon^{45,35}, Ph. Ghez⁴, V. Gibson⁴⁴, V.V. Gligorov³⁵, C. Göbel⁵⁴, D. Golubkov²⁸, A. Golutvin^{50,28,35}, A. Gomes², H. Gordon⁵², M. Grabalosa Gándara³³, R. Graciani Diaz³³, L.A. Granado Cardoso³⁵, E. Graugés³³, G. Graziani¹⁷, A. Grecu²⁶, E. Greening⁵², S. Gregson⁴⁴, O. Grünberg⁵⁵, B. Gui⁵³, E. Gushchin³⁰, Yu. Guz³², T. Gys³⁵, C. Hadjivasiliou⁵³, G. Haefeli³⁶, C. Haen³⁵, S.C. Haines⁴⁴, T. Hampson⁴³, S. Hansmann-Menzemer¹¹, N. Harnew⁵², S.T. Harnew⁴³, J. Harrison⁵¹, P.F. Harrison⁴⁵, T. Hartmann⁵⁵, J. He⁷, V. Heijne³⁸, K. Hennessy⁴⁹, P. Henrard⁵, J.A. Hernando Morata³⁴, E. van Herwijnen³⁵, E. Hicks⁴⁹, M. Hoballah⁵, P. Hopchev⁴, W. Hulsbergen³⁸, P. Hunt⁵², T. Huse⁴⁹, R.S. Huston¹², D. Hutchcroft⁴⁹, D. Hynds⁴⁸, V. Iakovenko⁴¹, P. Ilten¹², J. Imong⁴³, R. Jacobsson³⁵, A. Jaeger¹¹, M. Jahjah Hussein⁵, E. Jans³⁸, F. Jansen³⁸, P. Jaton³⁶, B. Jean-Marie⁷, F. Jing³, M. John⁵², D. Johnson⁵²,

C.R. Jones⁴⁴, B. Jost³⁵, M. Kaballo⁹, S. Kandybei⁴⁰, M. Karacson³⁵, T.M. Karbach⁹,
 J. Keaveney¹², I.R. Kenyon⁴², U. Kerzel³⁵, T. Ketel³⁹, A. Keune³⁶, B. Khanji⁶, Y.M. Kim⁴⁷,
 M. Knecht³⁶, O. Kochebina⁷, I. Komarov²⁹, R.F. Koopman³⁹, P. Koppenburg³⁸, M. Korolev²⁹,
 A. Kozlinskiy³⁸, L. Kravchuk³⁰, K. Kreplin¹¹, M. Kreps⁴⁵, G. Krocker¹¹, P. Krokovny³¹,
 F. Kruse⁹, M. Kucharczyk^{20,23,35,j}, V. Kudryavtsev³¹, T. Kvaratskheliya^{28,35}, V.N. La Thi³⁶,
 D. Lacarrere³⁵, G. Lafferty⁵¹, A. Lai¹⁵, D. Lambert⁴⁷, R.W. Lambert³⁹, E. Lanciotti³⁵,
 G. Lanfranchi¹⁸, C. Langenbruch³⁵, T. Latham⁴⁵, C. Lazzeroni⁴², R. Le Gac⁶,
 J. van Leerdam³⁸, J.-P. Lees⁴, R. Lefèvre⁵, A. Leflat^{29,35}, J. Lefrançois⁷, O. Leroy⁶,
 T. Lesiak²³, L. Li³, Y. Li³, L. Li Gioi⁵, M. Lieng⁹, M. Liles⁴⁹, R. Lindner³⁵, C. Linn¹¹, B. Liu³,
 G. Liu³⁵, J. von Loeben²⁰, J.H. Lopes², E. Lopez Asamar³³, N. Lopez-March³⁶, H. Lu³,
 J. Luisier³⁶, A. Mac Raighne⁴⁸, F. Machefert⁷, I.V. Machikhiliyan^{4,28}, F. Maciuc¹⁰,
 O. Maev^{27,35}, J. Magnin¹, S. Malde⁵², R.M.D. Mamunur³⁵, G. Manca^{15,d}, G. Mancinelli⁶,
 N. Mangiafave⁴⁴, U. Marconi¹⁴, R. Märki³⁶, J. Marks¹¹, G. Martellotti²², A. Martens⁸,
 L. Martin⁵², A. Martín Sánchez⁷, M. Martinelli³⁸, D. Martinez Santos³⁵, A. Massafferri¹,
 Z. Mathe¹², C. Matteuzzi²⁰, M. Matveev²⁷, E. Maurice⁶, A. Mazurov^{16,30,35}, J. McCarthy⁴²,
 G. McGregor⁵¹, R. McNulty¹², M. Meissner¹¹, M. Merk³⁸, J. Merkel⁹, D.A. Milanes¹³,
 M.-N. Minard⁴, J. Molina Rodriguez⁵⁴, S. Monteil⁵, D. Moran¹², P. Morawski²³,
 R. Mountain⁵³, I. Mous³⁸, F. Muheim⁴⁷, K. Müller³⁷, R. Muresan²⁶, B. Muryn²⁴, B. Muster³⁶,
 J. Mylroie-Smith⁴⁹, P. Naik⁴³, T. Nakada³⁶, R. Nandakumar⁴⁶, I. Nasteva¹, M. Needham⁴⁷,
 N. Neufeld³⁵, A.D. Nguyen³⁶, C. Nguyen-Mau^{36,o}, M. Nicol⁷, V. Niess⁵, N. Nikitin²⁹,
 T. Nikodem¹¹, A. Nomerotski^{52,35}, A. Novoselov³², A. Oblakowska-Mucha²⁴, V. Obraztsov³²,
 S. Oggero³⁸, S. Ogilvy⁴⁸, O. Okhrimenko⁴¹, R. Oldeman^{15,d,35}, M. Orlandea²⁶,
 J.M. Otalora Goicochea², P. Owen⁵⁰, B.K. Pal⁵³, A. Palano^{13,b}, M. Palutan¹⁸, J. Panman³⁵,
 A. Papanestis⁴⁶, M. Pappagallo⁴⁸, C. Parkes⁵¹, C.J. Parkinson⁵⁰, G. Passaleva¹⁷, G.D. Patel⁴⁹,
 M. Patel⁵⁰, G.N. Patrick⁴⁶, C. Patrignani^{19,i}, C. Pavel-Nicorescu²⁶, A. Pazos Alvarez³⁴,
 A. Pellegrino³⁸, G. Penso^{22,l}, M. Pepe Altarelli³⁵, S. Perazzini^{14,c}, D.L. Perego^{20,j},
 E. Perez Trigo³⁴, A. Pérez-Calero Yzquierdo³³, P. Perret⁵, M. Perrin-Terrin⁶, G. Pessina²⁰,
 A. Petrolini^{19,i}, A. Phan⁵³, E. Picatoste Olloqui³³, B. Pie Valls³³, B. Pietrzyk⁴, T. Pilarčík⁴⁵,
 D. Pinci²², S. Playfer⁴⁷, M. Plo Casasus³⁴, F. Polci⁸, G. Polok²³, A. Poluektov^{45,31},
 E. Polycarpo², D. Popov¹⁰, B. Popovici²⁶, C. Potterat³³, A. Powell⁵², J. Prisciandaro³⁶,
 V. Pugatch⁴¹, A. Puig Navarro³³, W. Qian⁵³, J.H. Rademacker⁴³, B. Rakotomiaramanana³⁶,
 M.S. Rangel², I. Raniuk⁴⁰, N. Rauschmayr³⁵, G. Raven³⁹, S. Redford⁵², M.M. Reid⁴⁵,
 A.C. dos Reis¹, S. Ricciardi⁴⁶, A. Richards⁵⁰, K. Rinnert⁴⁹, D.A. Roa Romero⁵, P. Robbe⁷,
 E. Rodrigues^{48,51}, F. Rodrigues², P. Rodriguez Perez³⁴, G.J. Rogers⁴⁴, S. Roiser³⁵,
 V. Romanovsky³², A. Romero Vidal³⁴, M. Rosello^{33,n}, J. Rouvinet³⁶, T. Ruf³⁵, H. Ruiz³³,
 G. Sabatino^{21,k}, J.J. Saborido Silva³⁴, N. Sagidova²⁷, P. Sail⁴⁸, B. Saitta^{15,d}, C. Salzmann³⁷,
 B. Sanmartin Sedes³⁴, M. Sannino^{19,i}, R. Santacesaria²², C. Santamarina Rios³⁴,
 R. Santinelli³⁵, E. Santovetti^{21,k}, M. Sapunov⁶, A. Sarti^{18,l}, C. Satriano^{22,m}, A. Satta²¹,
 M. Savrie^{16,e}, D. Savrina²⁸, P. Schaack⁵⁰, M. Schiller³⁹, H. Schindler³⁵, S. Schleich⁹,
 M. Schlupp⁹, M. Schmelling¹⁰, B. Schmidt³⁵, O. Schneider³⁶, A. Schopper³⁵, M.-H. Schune⁷,
 R. Schwemmer³⁵, B. Sciascia¹⁸, A. Sciubba^{18,l}, M. Seco³⁴, A. Semennikov²⁸, K. Senderowska²⁴,
 I. Sepp⁵⁰, N. Serra³⁷, J. Serrano⁶, P. Seyfert¹¹, M. Shapkin³², I. Shapoval^{40,35}, P. Shatalov²⁸,
 Y. Shcheglov²⁷, T. Shears⁴⁹, L. Shekhtman³¹, O. Shevchenko⁴⁰, V. Shevchenko²⁸, A. Shires⁵⁰,
 R. Silva Coutinho⁴⁵, T. Skwarnicki⁵³, N.A. Smith⁴⁹, E. Smith^{52,46}, M. Smith⁵¹, K. Sobczak⁵,
 F.J.P. Soler⁴⁸, A. Solomin⁴³, F. Soomro^{18,35}, D. Souza⁴³, B. Souza De Paula², B. Spaan⁹,
 A. Sparkes⁴⁷, P. Spradlin⁴⁸, F. Stagni³⁵, S. Stahl¹¹, O. Steinkamp³⁷, S. Stoica²⁶, S. Stone^{53,35},

B. Storaci³⁸, M. Straticiuc²⁶, U. Straumann³⁷, V.K. Subbiah³⁵, S. Swientek⁹,
M. Szczekowski²⁵, P. Szczypka³⁶, T. Szumlak²⁴, S. T'Jampens⁴, M. Teklishyn⁷,
E. Teodorescu²⁶, F. Teubert³⁵, C. Thomas⁵², E. Thomas³⁵, J. van Tilburg¹¹, V. Tisserand⁴,
M. Tobin³⁷, S. Tolk³⁹, S. Topp-Joergensen⁵², N. Torr⁵², E. Tournefier^{4,50}, S. Tourneur³⁶,
M.T. Tran³⁶, A. Tsaregorodtsev⁶, N. Tuning³⁸, M. Ubeda Garcia³⁵, A. Ukleja²⁵, U. Uwer¹¹,
V. Vagnoni¹⁴, G. Valenti¹⁴, R. Vazquez Gomez³³, P. Vazquez Regueiro³⁴, S. Vecchi¹⁶,
J.J. Velthuis⁴³, M. Veltre^{17,g}, G. Veneziano³⁶, M. Vesterinen³⁵, B. Viaud⁷, I. Videau⁷,
D. Vieira², X. Vilasis-Cardona^{33,n}, J. Visniakov³⁴, A. Vollhardt³⁷, D. Volyanskyy¹⁰,
D. Voong⁴³, A. Vorobyev²⁷, V. Vorobyev³¹, C. Voß⁵⁵, H. Voss¹⁰, R. Waldi⁵⁵, R. Wallace¹²,
S. Wandernoth¹¹, J. Wang⁵³, D.R. Ward⁴⁴, N.K. Watson⁴², A.D. Webber⁵¹, D. Websdale⁵⁰,
M. Whitehead⁴⁵, J. Wicht³⁵, D. Wiedner¹¹, L. Wiggers³⁸, G. Wilkinson⁵², M.P. Williams^{45,46},
M. Williams⁵⁰, F.F. Wilson⁴⁶, J. Wishahi⁹, M. Witek²³, W. Witzeling³⁵, S.A. Wotton⁴⁴,
S. Wright⁴⁴, S. Wu³, K. Wyllie³⁵, Y. Xie⁴⁷, F. Xing⁵², Z. Xing⁵³, Z. Yang³, R. Young⁴⁷,
X. Yuan³, O. Yushchenko³², M. Zangoli¹⁴, M. Zavertyaev^{10,a}, F. Zhang³, L. Zhang⁵³,
W.C. Zhang¹², Y. Zhang³, A. Zhelezov¹¹, L. Zhong³, A. Zvyagin³⁵.

¹*Centro Brasileiro de Pesquisas Físicas (CBPF), Rio de Janeiro, Brazil*

²*Universidade Federal do Rio de Janeiro (UFRJ), Rio de Janeiro, Brazil*

³*Center for High Energy Physics, Tsinghua University, Beijing, China*

⁴*LAPP, Université de Savoie, CNRS/IN2P3, Annecy-Le-Vieux, France*

⁵*Clermont Université, Université Blaise Pascal, CNRS/IN2P3, LPC, Clermont-Ferrand, France*

⁶*CPPM, Aix-Marseille Université, CNRS/IN2P3, Marseille, France*

⁷*LAL, Université Paris-Sud, CNRS/IN2P3, Orsay, France*

⁸*LPNHE, Université Pierre et Marie Curie, Université Paris Diderot, CNRS/IN2P3, Paris, France*

⁹*Fakultät Physik, Technische Universität Dortmund, Dortmund, Germany*

¹⁰*Max-Planck-Institut für Kernphysik (MPIK), Heidelberg, Germany*

¹¹*Physikalisches Institut, Ruprecht-Karls-Universität Heidelberg, Heidelberg, Germany*

¹²*School of Physics, University College Dublin, Dublin, Ireland*

¹³*Sezione INFN di Bari, Bari, Italy*

¹⁴*Sezione INFN di Bologna, Bologna, Italy*

¹⁵*Sezione INFN di Cagliari, Cagliari, Italy*

¹⁶*Sezione INFN di Ferrara, Ferrara, Italy*

¹⁷*Sezione INFN di Firenze, Firenze, Italy*

¹⁸*Laboratori Nazionali dell'INFN di Frascati, Frascati, Italy*

¹⁹*Sezione INFN di Genova, Genova, Italy*

²⁰*Sezione INFN di Milano Bicocca, Milano, Italy*

²¹*Sezione INFN di Roma Tor Vergata, Roma, Italy*

²²*Sezione INFN di Roma La Sapienza, Roma, Italy*

²³*Henryk Niewodniczanski Institute of Nuclear Physics Polish Academy of Sciences, Kraków, Poland*

²⁴*AGH University of Science and Technology, Kraków, Poland*

²⁵*Soltan Institute for Nuclear Studies, Warsaw, Poland*

²⁶*Horia Hulubei National Institute of Physics and Nuclear Engineering, Bucharest-Magurele, Romania*

²⁷*Petersburg Nuclear Physics Institute (PNPI), Gatchina, Russia*

²⁸*Institute of Theoretical and Experimental Physics (ITEP), Moscow, Russia*

²⁹*Institute of Nuclear Physics, Moscow State University (SINP MSU), Moscow, Russia*

³⁰*Institute for Nuclear Research of the Russian Academy of Sciences (INR RAN), Moscow, Russia*

³¹*Budker Institute of Nuclear Physics (SB RAS) and Novosibirsk State University, Novosibirsk, Russia*

³²*Institute for High Energy Physics (IHEP), Protvino, Russia*

³³*Universitat de Barcelona, Barcelona, Spain*

³⁴*Universidad de Santiago de Compostela, Santiago de Compostela, Spain*

- ³⁵European Organization for Nuclear Research (CERN), Geneva, Switzerland
³⁶Ecole Polytechnique Fédérale de Lausanne (EPFL), Lausanne, Switzerland
³⁷Physik-Institut, Universität Zürich, Zürich, Switzerland
³⁸Nikhef National Institute for Subatomic Physics, Amsterdam, The Netherlands
³⁹Nikhef National Institute for Subatomic Physics and VU University Amsterdam, Amsterdam, The Netherlands
⁴⁰NSC Kharkiv Institute of Physics and Technology (NSC KIPT), Kharkiv, Ukraine
⁴¹Institute for Nuclear Research of the National Academy of Sciences (KINR), Kyiv, Ukraine
⁴²University of Birmingham, Birmingham, United Kingdom
⁴³H.H. Wills Physics Laboratory, University of Bristol, Bristol, United Kingdom
⁴⁴Cavendish Laboratory, University of Cambridge, Cambridge, United Kingdom
⁴⁵Department of Physics, University of Warwick, Coventry, United Kingdom
⁴⁶STFC Rutherford Appleton Laboratory, Didcot, United Kingdom
⁴⁷School of Physics and Astronomy, University of Edinburgh, Edinburgh, United Kingdom
⁴⁸School of Physics and Astronomy, University of Glasgow, Glasgow, United Kingdom
⁴⁹Oliver Lodge Laboratory, University of Liverpool, Liverpool, United Kingdom
⁵⁰Imperial College London, London, United Kingdom
⁵¹School of Physics and Astronomy, University of Manchester, Manchester, United Kingdom
⁵²Department of Physics, University of Oxford, Oxford, United Kingdom
⁵³Syracuse University, Syracuse, NY, United States
⁵⁴Pontifícia Universidade Católica do Rio de Janeiro (PUC-Rio), Rio de Janeiro, Brazil, associated to ²
⁵⁵Institut für Physik, Universität Rostock, Rostock, Germany, associated to ¹¹
- ^aP.N. Lebedev Physical Institute, Russian Academy of Science (LPI RAS), Moscow, Russia
^bUniversità di Bari, Bari, Italy
^cUniversità di Bologna, Bologna, Italy
^dUniversità di Cagliari, Cagliari, Italy
^eUniversità di Ferrara, Ferrara, Italy
^fUniversità di Firenze, Firenze, Italy
^gUniversità di Urbino, Urbino, Italy
^hUniversità di Modena e Reggio Emilia, Modena, Italy
ⁱUniversità di Genova, Genova, Italy
^jUniversità di Milano Bicocca, Milano, Italy
^kUniversità di Roma Tor Vergata, Roma, Italy
^lUniversità di Roma La Sapienza, Roma, Italy
^mUniversità della Basilicata, Potenza, Italy
ⁿLIFAELS, La Salle, Universitat Ramon Llull, Barcelona, Spain
^oHanoi University of Science, Hanoi, Viet Nam

Interpretations of measurements of time-dependent CP violation in $B_s^0 \rightarrow J/\psi\phi$ and $B_s^0 \rightarrow J/\psi f_0(980)$ decays have thus far assumed the dominance of the colour-suppressed tree-level process. However, there are contributions from higher order (penguin) processes (see Fig. 1) that cannot be calculated reliably in QCD and could be large enough to affect the measured asymmetries. It has been suggested that the penguin effects can be determined by means of an analysis of the angular distribution of $B_s^0 \rightarrow J/\psi\bar{K}^*(892)^0$, where the penguin diagram is not suppressed relative to the tree-level one, and $SU(3)$ flavour symmetry arguments can be used to determine the hadronic parameters entering the $B_s^0 \rightarrow J/\psi\phi$ observables [1].

In this paper the $K^*(892)^0$ meson will be written as K^{*0} , while for other K^* resonances the mass will be given in parentheses. Furthermore, mention of any specific mode implies the use of the charge conjugated mode as well, and $K^-\pi^+$ pairs will be simply written as $K\pi$. The decay $B_s^0 \rightarrow J/\psi\bar{K}^{*0}$ has already been observed by the CDF experiment [2], which reported $\mathcal{B}(B_s^0 \rightarrow J/\psi\bar{K}^{*0}) = (8.3 \pm 3.8) \times 10^{-5}$. Under the assumption that the light quark (s,d) is a spectator of the b quark decay, the branching fraction can be approximated as

$$\mathcal{B}(B_s^0 \rightarrow J/\psi\bar{K}^{*0}) \sim \frac{|V_{cd}|^2}{|V_{cs}|^2} \times \mathcal{B}(B^0 \rightarrow J/\psi K^{*0}) = (6.5 \pm 1.0) \times 10^{-5}, \quad (1)$$

with $|V_{cd}| = 0.230 \pm 0.011$, $|V_{cs}| = 1.023 \pm 0.036$ [3], and $\mathcal{B}(B^0 \rightarrow J/\psi K^{*0}) = (1.29 \pm 0.05 \pm 0.13) \times 10^{-3}$ [4]. The measurement in Ref. [4], where the $K\pi$ S-wave contribution is subtracted, is used instead of the PDG average.

In this paper, 0.37 fb^{-1} of data taken in 2011 are used to determine $\mathcal{B}(B_s^0 \rightarrow J/\psi\bar{K}^{*0})$, to study the angular properties of the decay products of the B_s^0 meson, and to measure the resonant contributions to the $K\pi$ spectrum in the region of the K^{*0} meson. The measurement of the branching fraction uses the decay $B^0 \rightarrow J/\psi K^{*0}$ as a normalization mode.

The LHCb detector [5] is a single-arm forward spectrometer covering the pseudo-rapidity range $2 < \eta < 5$. The detector includes a high precision tracking system consisting of a silicon-strip vertex detector located around the interaction point, a large-area silicon-strip detector located upstream of a dipole magnet with a bending power of about 4 Tm , and three stations of silicon-strip detectors and straw drift tubes placed down-

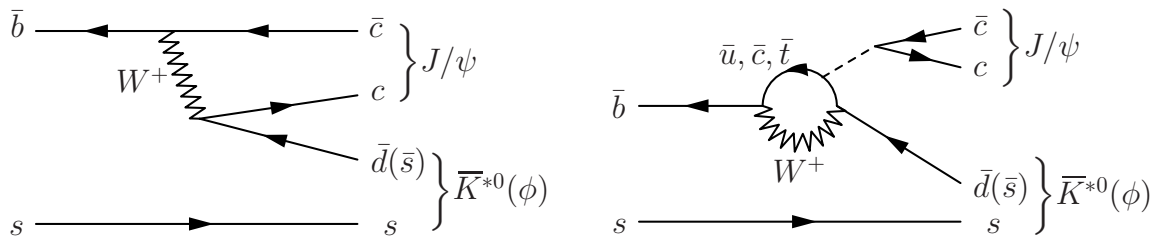


Figure 1: Tree and penguin decay topologies contributing to the decays $B_s^0 \rightarrow J/\psi\bar{K}^{*0}$ and $B_s^0 \rightarrow J/\psi\phi$. The dashed line indicates a colour singlet exchange.

stream. The combined tracking system has a momentum resolution $\Delta p/p$ that varies from 0.4% at $5\text{ GeV}/c$ to 0.6% at $100\text{ GeV}/c$. Two ring-imaging Cherenkov detectors (RICH) are used to determine the identity of charged particles. The separation of pions and kaons is such that, for efficiencies of $\sim 75\%$ the rejection power is above 99%. Photon, electron and hadron candidates are identified by a calorimeter system consisting of scintillating-pad and pre-shower detectors, an electromagnetic calorimeter and a hadronic calorimeter. Muons are identified by alternating layers of iron and multiwire proportional chambers.

The trigger consists of a hardware stage, based on information from the calorimeter and muon systems, followed by a software stage called High Level Trigger (HLT) that applies a full event reconstruction. Events with muon final states are triggered using two hardware trigger decisions: the single-muon decision (one muon candidate with transverse momentum $p_T > 1.5\text{ GeV}/c$), and the di-muon decision (two muon candidates with $p_{T,1}$ and $p_{T,2}$ such that $\sqrt{p_{T,1}p_{T,2}} > 1.3\text{ GeV}/c$). All tracks in the HLT are required to have a $p_T > 0.5\text{ GeV}/c$. The single muon trigger decision in the HLT selects events with at least one muon track with an impact parameter $\text{IP} > 0.1\text{ mm}$ with respect to the primary vertex and $p_T > 1.0\text{ GeV}/c$. The di-muon trigger decision, designed to select J/ψ mesons, also requires a di-muon mass ($M_{\mu\mu}$) $2970 < M_{\mu\mu} < 3210\text{ MeV}/c^2$.

Simulated events are used to compute detection efficiencies and angular acceptances. For this purpose, pp collisions are generated using PYTHIA 6.4 [6] with a specific LHCb configuration [7]. Decays of hadronic particles are described by EvtGen [8] in which final state radiation is generated using PHOTOS [9]. The interaction of the generated particles with the detector and its response are implemented using the GEANT4 toolkit [10] as described in Ref. [11].

The selection of $B_{(s)}^0 \rightarrow J/\psi K^{*0}$ decays first requires the reconstruction of a $J/\psi \rightarrow \mu^+\mu^-$ candidate. The J/ψ vertex is required to be separated from any primary vertex (PV) by a distance-of-flight significance greater than 13. Subsequently, the muons from the J/ψ decay are combined with the K and π candidates to form a good vertex, where the di-muon mass is constrained to the J/ψ mass. A $p_T > 0.5\text{ GeV}/c$ is required for each of the four daughter tracks. Positive muon identification is required for the two tracks of the J/ψ decay, and the kaons and pions are selected using the different hadron probabilities based on combined information given by the RICH detectors. The candidate $B_{(s)}^0$ momentum is required to be compatible with the flight direction as given by the vector connecting the PV with the candidate vertex. An explicit veto to remove $B^+ \rightarrow J/\psi K^+$ events is applied, as they otherwise would pollute the upper sideband of the $B_{(s)}^0$ mass spectrum.

Following this initial selection, several geometrical variables are combined into a single discriminant geometrical likelihood variable (GL). This multivariate method is described in Refs. [12,13]. The geometrical variables chosen to build the GL are: the $B_{(s)}^0$ candidate minimum impact parameter with respect to any PV in the event, the decay time of the $B_{(s)}^0$ candidate, the minimum impact parameter χ^2 of the four daughter tracks with respect to all PV in the event (defined as the difference between the χ^2 of the PV built with and without the considered track), the distance of closest approach between the J/ψ and K^{*0}

trajectories reconstructed from their decay products, and the p_T of the $B_{(s)}^0$ candidate. The GL was tuned using simulated $B^0 \rightarrow J/\psi K^{*0}$ signal passing the selection criteria, and background from data in the $B_{(s)}^0$ mass sidebands with a value for the kaon particle identification variable in a range which does not overlap with the one used to select the data sample for the final analysis.

The $K\pi$ mass spectrum in the $B^0 \rightarrow J/\psi K\pi$ channel is dominated by the K^{*0} resonance but contains a non-negligible S-wave contribution, originating from $K_0^*(1430)^0$ and non-resonant $K\pi$ pairs [14]. To determine $\mathcal{B}(B_s^0 \rightarrow J/\psi \bar{K}^{*0})$ it is therefore important to measure the S-wave magnitude in both $B_{(s)}^0 \rightarrow J/\psi K\pi$ channels. The $K\pi$ spectrum is analyzed in terms of a non-resonant S-wave and several $K\pi$ resonances parameterized using relativistic Breit-Wigner distributions with mass-dependent widths, following closely [14]. The considered waves are: a non-resonant S-wave amplitude interfering with the $K_0^*(1430)^0$ resonance, K^{*0} for the P-wave and $K_2^*(1430)^0$ for the D-wave. F-wave and G-wave components are found to be negligible in the B^0 fit. In bins of the $K\pi$ mass, a fit is made to the $B_{(s)}^0$ candidate mass distribution to determine the yield. As shown in Fig. 2, a fit is then made to the B^0 and B_s^0 yields as a function of the $K\pi$ mass without any efficiency correction. The S and P-wave components dominate in the ± 40 MeV/ c^2 window around the K^{*0} mass, where the K^{*0} contribution is above 90%. A more exact determination of this contribution using this method would require $K\pi$ mass-dependent angular acceptance corrections. For the branching fraction calculation, the fraction of K^{*0} candidates is determined from a different full angular and mass fit, which is described next.

The angular and mass analysis is based on an unbinned maximum likelihood fit which handles simultaneously the mass ($M_{J/\psi K\pi}$) and the angular parameters of the $B_{(s)}^0$ decays and the background. Each of these three components is modelled as a product of probability density functions (PDF), $\mathcal{P}(M_{J/\psi K\pi}, \psi, \theta, \varphi) = \mathcal{P}(M_{J/\psi K\pi}) \mathcal{P}(\psi, \theta, \varphi)$, with ψ the angle between the kaon momentum in the rest frame of the K^{*0} and the direction of motion of the K^{*0} in the rest frame of the B . The polar and azimuthal angles (θ, φ) describe the direction of the μ^+ in the coordinate system defined in the J/ψ rest frame, where the x axis is the direction of motion of the $B_{(s)}^0$ meson, the z axis is normal to the plane formed by the x axis and the kaon momentum, and the y axis is chosen so that the y component of the kaon momentum is positive.

The function describing the mass distribution of both $B_{(s)}^0$ signal peaks is the sum of two Crystal Ball (CB) functions [16], which are a combination of a Gaussian and a power law function to describe the radiative tail at low masses,

$$\mathcal{P}(M_{J/\psi K\pi}) = f \text{CB}(M_{J/\psi K\pi}, \mu_B, \sigma_1, \alpha_1) + (1 - f) \text{CB}(M_{J/\psi K\pi}, \mu_B, \sigma_2, \alpha_2). \quad (2)$$

The starting point of the radiative tail is governed by a transition point parameter $\alpha_{(1,2)}$. The mean and width of the Gaussian component are μ_B and $\sigma_{(1,2)}$. The values of the f , σ_1 , σ_2 , α_1 and α_2 parameters are constrained to be the same for the B_s^0 and B^0 peaks. The difference in the means between the B_s^0 and the B^0 distributions, $(\mu_{B_s^0} - \mu_{B^0})$, is fixed to the value taken from Ref. [17]. The mass PDF of the background is described by an exponential function.

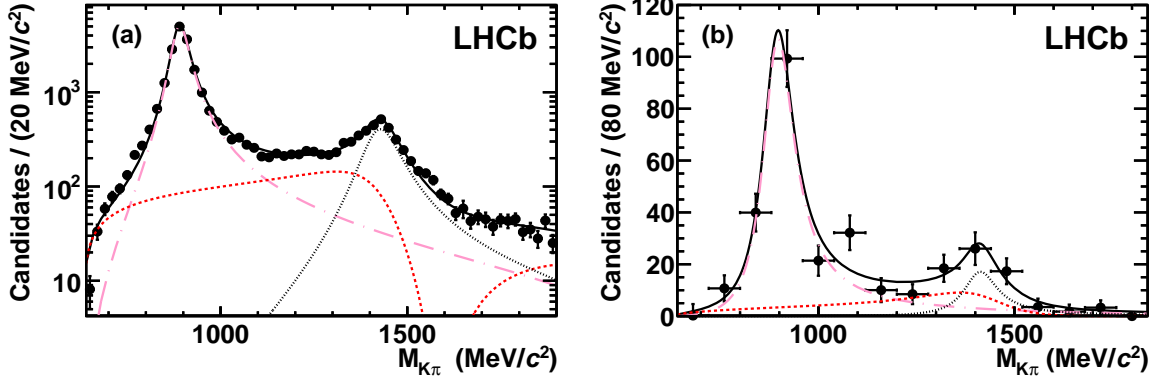


Figure 2: Fit to the $K\pi$ mass spectrum for (a) $B^0 \rightarrow J/\psi K\pi$ events, and (b) $B_s^0 \rightarrow J/\psi K\pi$ events. The $B_{(s)}^0 \rightarrow J/\psi K\pi$ yields in each bin of $K\pi$ mass are determined from a fit to the $J/\psi K\pi$ mass spectrum. The pink dashed-dotted line represents the K^{*0} , the red short-dashed line is the S-wave and the black dotted line is the $K_2^*(1430)$. The black solid line is their sum.

Assuming that direct CP violation and the $B_{(s)}^0 - \bar{B}_{(s)}^0$ production asymmetry are insignificant, the differential decay rate is [1, 15]

$$\begin{aligned}
\frac{d^3\Gamma}{d\Omega} \propto & 2|A_0|^2 \cos^2 \psi (1 - \sin^2 \theta \cos^2 \varphi) \\
& + |A_{||}|^2 \sin^2 \psi (1 - \sin^2 \theta \sin^2 \varphi) \\
& + |A_{\perp}|^2 \sin^2 \psi \sin^2 \theta \\
& + \frac{1}{\sqrt{2}} |A_0| |A_{||}| \cos(\delta_{||} - \delta_0) \sin 2\psi \sin^2 \theta \sin 2\varphi \\
& + \frac{2}{3} |A_S|^2 [1 - \sin^2 \theta \cos^2 \varphi] \\
& + \frac{4\sqrt{3}}{3} |A_0| |A_S| \cos(\delta_S - \delta_0) \cos \psi [1 - \sin^2 \theta \cos^2 \varphi] \\
& + \frac{\sqrt{6}}{3} |A_{||}| |A_S| \cos(\delta_{||} - \delta_S) \sin \psi \sin^2 \theta \sin 2\varphi,
\end{aligned} \tag{3}$$

where A_0 , $A_{||}$ and A_{\perp} are the decay amplitudes corresponding to longitudinally and transversely polarized vector mesons. $A_S = |A_S| e^{i\delta_S}$ is the $K\pi$ S-wave amplitude and $(\delta_{||} - \delta_0)$ the relative phase between the longitudinal and parallel amplitudes. The convention $\delta_0 = 0$ is used hereafter. The Ω differential is $d\Omega \equiv d\cos \psi d\cos \theta d\varphi$. The polarization fractions are normalized according to

$$f_{L,||,\perp} = \frac{|A_{0,||,\perp}|^2}{|A_0|^2 + |A_{||}|^2 + |A_{\perp}|^2}, \tag{4}$$

which satisfy $f_L + f_{||} + f_{\perp} = 1$.

The parameters f_L , f_{\parallel} and δ_{\parallel} describing the P-wave are left floating in the fit. The $|A_S|$ amplitude and the δ_S phase depend on $M_{K\pi}$, but this dependence is ignored in the fit, which is performed in a $K\pi$ mass window of $\pm 40 \text{ MeV}/c^2$, and they are just treated also as floating parameters. A systematic uncertainty is later associated with this assumption. The angular distribution of observed events is parameterized as a product of the expression in Eq. 3 and a detector acceptance function, $\text{Acc}(\Omega)$, which describes the efficiency to trigger, reconstruct and select the events. Simulation studies have shown almost no correlation between the three one-dimensional angular acceptances $\text{Acc}_\psi(\psi)$, $\text{Acc}_\theta(\theta)$ and $\text{Acc}_\phi(\varphi)$. Therefore the global acceptance factorizes as $\text{Acc}(\Omega) = \text{Acc}_\psi(\psi) \text{Acc}_\theta(\theta) \text{Acc}_\phi(\varphi)$, where $\text{Acc}_\psi(\psi)$ is parameterized as a fifth degree polynomial, $\text{Acc}_\theta(\theta)$ as a second degree polynomial and $\text{Acc}_\phi(\phi)$ as a sinusoidal function. A systematic uncertainty due to this factorization hypothesis is later evaluated. The angular distribution for the background component is determined using the upper sideband of the B_s^0 mass spectrum, defined as the interval [5417, 5779] MeV/c^2 .

Figure 3 shows the projection of the fit in the $M_{J/\psi K\pi}$ mass axis, together with the projections in the angular variables in a window of $\pm 25 \text{ MeV}/c^2$ around the B_s^0 mass. The number of candidates corresponding to B^0 and B_s^0 decays is found to be $13,365 \pm 116$ and 114 ± 11 , respectively.

Table 1: Summary of the measured $B_s^0 \rightarrow J/\psi \bar{K}^{*0}$ angular properties and their statistical and systematic uncertainties.

Parameter name	$ A_S ^2$	f_L	f_{\parallel}
Value and statistical error	$0.07^{+0.15}_{-0.07}$	0.50 ± 0.08	$0.19^{+0.10}_{-0.08}$
Systematic uncertainties			
Angular acceptance	0.044	0.011	0.016
Background angular model	0.038	0.017	0.013
Assumption $\delta_S(M_{K\pi}) = \text{constant}$	0.026	0.005	0.002
B^0 contamination	0.036	0.004	0.007
Fit bias	—	—	0.005
Total systematic error	0.073	0.021	0.022

Tables 1 and 2 summarize the measurements of the $B_{(s)}^0 \rightarrow J/\psi \bar{K}^{*0}$ angular parameters, together with their statistical and systematic uncertainties. The correlation coefficient given by the fit between f_L and f_{\parallel} is $\rho = -0.44$ for B_s^0 decays. The results for the $B^0 \rightarrow J/\psi \bar{K}^{*0}$ decay are in good agreement with previous measurements [4, 15, 18, 19].

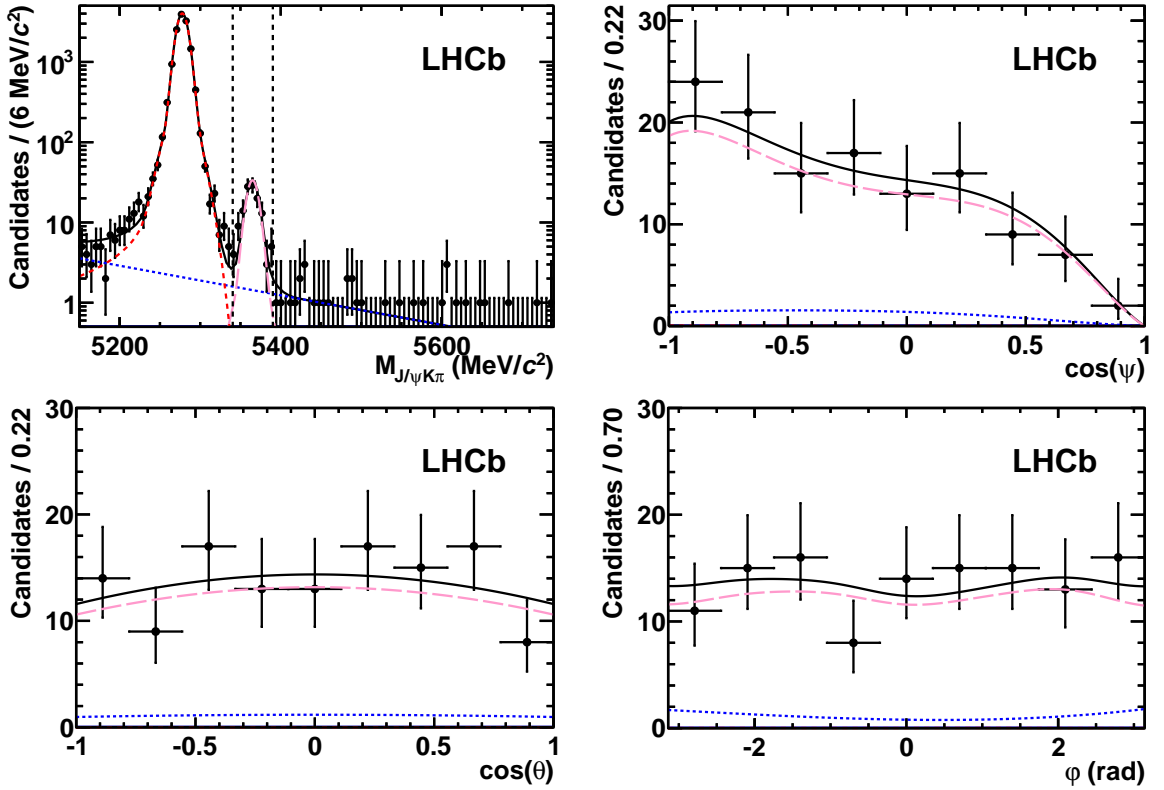


Figure 3: Projections of the fit in $M_{J/\psi K\pi}$ and in the angular variables for the mass range indicated by the two dashed vertical lines in the mass plot. The red dashed, pink long-dashed, and blue dotted lines represent the fitted contributions from $B^0 \rightarrow J/\psi K^{*0}$, $B_s^0 \rightarrow J/\psi \bar{K}^{*0}$ and background. The black solid line is their sum.

Based on this agreement, the systematic uncertainties caused by the modelling of the angular acceptance were evaluated by summing in quadrature the statistical error on

Table 2: Angular parameters of $B^0 \rightarrow J/\psi K^{*0}$ needed to compute $\mathcal{B}(B_s^0 \rightarrow J/\psi \bar{K}^{*0})$. The systematic uncertainties from background modelling and the mass PDF are found to be negligible in this case.

Parameter name	$ A_S ^2$	f_L	$f_{ }$
Value and statistical error	0.037 ± 0.010	0.569 ± 0.007	0.240 ± 0.009
Systematic uncertainties			
Angular acceptance	0.044	0.011	0.016
Assumption $\delta_S(M_{K\pi}) = \text{constant}$	0.026	0.005	0.002
Total systematic error	0.051	0.012	0.016

the measured $B^0 \rightarrow J/\psi K^{*0}$ parameters with the uncertainties on the world averages ($f_L = 0.570 \pm 0.008$ and $f_{\perp} = 0.219 \pm 0.010$) [3]. The angular analysis was repeated with two additional acceptance descriptions, one which uses a three-dimensional histogram to describe the efficiency avoiding any factorization hypothesis, and another one based on a method of normalization weights described in Ref. [20]. A very good agreement was found in the values of the polarization fractions computed with all the three methods. For the parameter $|A_S|^2$, uncertainties caused by the finite size of the simulation sample used for the acceptance description, as well as from the studies with several acceptance models, are included. The systematic uncertainty caused by the choice of the angular PDF for the background is shown for the $B_s^0 \rightarrow J/\psi \bar{K}^{*0}$ decay but it was found to be negligible for $B^0 \rightarrow J/\psi K^{*0}$.

Also included in Tables 1 and 2 is the uncertainty from the assumption of a constant δ_S as a function of $M_{K\pi}$. This assumption can be relaxed by adding an extra free parameter to the angular PDF. This addition makes the fit unstable for the small size of the B_s^0 sample, but can be used in the control channel $B^0 \rightarrow J/\psi K^{*0}$. The differences found in the B^0 parameters with the two alternate parameterizations are used as systematic uncertainties. The parameters δ_{\parallel} fit to $\cos(\delta_{\parallel}) = -0.960^{+0.021}_{-0.017}$ for the B^0 and to $\cos(\delta_{\parallel}) = -0.93 \pm 0.31$ (where the error corresponds to the positive one, being symmetrized) for the B_s^0 . These parameters could in principle affect the efficiency corrections, but it was found that the effect of different values of δ_{\parallel} on the overall efficiency is negligible. A simulation study of the fit pulls has shown that the errors on f_L and f_{\parallel} of the B_s^0 decays are overestimated by a small amount ($\sim 10\%$) since they do not follow exactly a Gaussian distribution, therefore the decision was taken to quote an uncertainty which corresponds to an interval containing 68% of the generated experiments, rather than giving an error corresponding to a log-likelihood interval of 0.5. A slight bias observed in the pulls of f_{\parallel} in B_s^0 decays was accounted for by adding a systematic uncertainty corresponding to 6% of the statistical error.

The ratio of the two branching fractions is obtained from

$$\frac{\mathcal{B}(B_s^0 \rightarrow J/\psi \bar{K}^{*0})}{\mathcal{B}(B^0 \rightarrow J/\psi K^{*0})} = \frac{f_d}{f_s} \frac{\varepsilon_{B^0}^{\text{tot}}}{\varepsilon_{B_s^0}^{\text{tot}}} \frac{\lambda_{B^0}}{\lambda_{B_s^0}} \frac{f_{K^{*0}}^{(d)}}{f_{K^{*0}}^{(s)}} \frac{N_{B_s^0}}{N_{B^0}}, \quad (5)$$

where f_d (f_s) is the probability of the b quark to hadronize to B^0 (B_s^0) mesons, $\varepsilon_{B^0}^{\text{tot}}/\varepsilon_{B_s^0}^{\text{tot}}$ is the efficiency ratio, $\lambda_{B^0}/\lambda_{B_s^0}$ is the ratio of angular corrections, $f_{K^{*0}}^{(s)}/f_{K^{*0}}^{(d)}$ is the ratio of K^{*0} fractions and $N_{B_s^0}/N_{B^0}$ is the ratio of signal yields. The value of f_d/f_s has been taken from Ref. [21]. The efficiencies in the ratio $\varepsilon_{B^0}^{\text{tot}}/\varepsilon_{B_s^0}^{\text{tot}}$ are computed using simulation and receive two contributions: the efficiency of the offline reconstruction (including geometrical acceptance) and selection cuts, and the trigger efficiency on events that satisfy the analysis offline selection criteria. The systematic uncertainty in the efficiency ratio is negligible due to the similarity of the final states. Effects due to possible differences in the decay time acceptance between data and simulation were found to affect the efficiency ratio by less than 1 per mille. On the other hand, since the efficiency depends on the angular distribution of the decay products, correction factors λ_{B^0} and $\lambda_{B_s^0}$ are applied to account

Table 3: Parameter values and errors for $\frac{\mathcal{B}(B_s^0 \rightarrow J/\psi \bar{K}^{*0})}{\mathcal{B}(B^0 \rightarrow J/\psi K^{*0})}$.

Parameter	Name	Value
Hadronization fractions	f_d/f_s	3.75 ± 0.29
Efficiency ratio	$\varepsilon_{B^0}^{\text{tot}}/\varepsilon_{B_s^0}^{\text{tot}}$	0.97 ± 0.01
Angular corrections	$\lambda_{B^0}/\lambda_{B_s^0}$	1.01 ± 0.04
Ratio of K^{*0} fractions	$f_{K^{*0}}^{(s)}/f_{K^{*0}}^{(d)}$	1.09 ± 0.08
B signal yields	$N_{B_s^0}/N_{B^0}$	$(8.5^{+0.9}_{-0.8} \pm 0.8) \times 10^{-3}$

for the difference between the angular amplitudes used in simulation and those measured in the data. The observed numbers of B^0 and B_s^0 decays, denoted by N_{B^0} and $N_{B_s^0}$, correspond to the number of $B_s^0 \rightarrow J/\psi K\pi$ and $B^0 \rightarrow J/\psi K\pi$ decays with a $K\pi$ mass in a ± 40 MeV/ c^2 window around the nominal K^{*0} mass. This includes mostly the K^{*0} meson, but also an S-wave component and the interference between the S-wave and P-wave components. The fraction of candidates with a K^{*0} meson present is then

$$f_{K^{*0}} = \frac{\int_{\Omega} \text{Acc}(\Omega) \left. \frac{d^3\Gamma}{d\Omega} \right|_{|A_S|=0} d\Omega}{\int_{\Omega} \text{Acc}(\Omega) \frac{d^3\Gamma}{d\Omega} d\Omega}, \quad (6)$$

from which the ratio $f_{K^{*0}}^{(s)}/f_{K^{*0}}^{(d)} = 1.09 \pm 0.08$ follows. Table 3 summarizes all the numbers needed to compute the ratio of branching fractions

$$\frac{\mathcal{B}(B_s^0 \rightarrow J/\psi \bar{K}^{*0})}{\mathcal{B}(B^0 \rightarrow J/\psi K^{*0})} = (3.43^{+0.34}_{-0.36} \pm 0.50)\%.$$

The contributions to the systematic uncertainty are also listed in Table 3 and their relative magnitudes are: 1.2% for the error in the efficiency ratio; 2.5% for the uncertainty on the transition point (α) of the Crystal Ball function; 8.6% for the parameterization of the upper tail of the B^0 peak; 3.9% for the angular correction of the efficiencies; 7.3% for the uncertainty on the ratio $f_{K^{*0}}^{(s)}/f_{K^{*0}}^{(d)}$ and 7.7% for the uncertainty on f_d/f_s . The errors are added in quadrature.

Taking the value $\mathcal{B}(B^0 \rightarrow J/\psi K^{*0}) = (1.29 \pm 0.05 \pm 0.13) \times 10^{-3}$ from Ref. [4] the following branching fraction is obtained,

$$\mathcal{B}(B_s^0 \rightarrow J/\psi \bar{K}^{*0}) = (4.4^{+0.5}_{-0.4} \pm 0.8) \times 10^{-5}.$$

This value is compatible with the CDF measurement [2] and is similar to the naive quark spectator model prediction of Eq. (1), although it is closer to the estimation in Ref. [1], $\mathcal{B}(B_s^0 \rightarrow J/\psi \bar{K}^{*0}) \sim 2 \times \mathcal{B}(B_d^0 \rightarrow J/\psi \rho^0) = (4.6 \pm 0.4) \times 10^{-5}$. The branching fraction measured here is in fact the average of the $B_s^0 \rightarrow J/\psi \bar{K}^{*0}$ and $\bar{B}_s^0 \rightarrow J/\psi K^{*0}$ branching

fractions and corresponds to the time integrated quantity, while theory predictions usually refer to the branching fraction at $t = 0$ [22]. In the case of $B_s^0 \rightarrow J/\psi \bar{K}^{*0}$, the two differ by $(\Delta\Gamma_s/2\Gamma_s)^2 = (0.77 \pm 0.25)\%$, where $\Delta\Gamma_s = \Gamma_L - \Gamma_H$, $\Gamma_s = (\Gamma_L + \Gamma_H)/2$, and $\Gamma_{L(H)}$ is the decay width of the light (heavy) B_s^0 -mass eigenstate.

In conclusion, using 0.37 fb^{-1} of pp collisions collected by the LHCb detector at $\sqrt{s} = 7 \text{ TeV}$, a measurement of the $B_s^0 \rightarrow J/\psi \bar{K}^{*0}$ branching fraction yields $\mathcal{B}(B_s^0 \rightarrow J/\psi \bar{K}^{*0}) = (4.4_{-0.4}^{+0.5} \pm 0.8) \times 10^{-5}$. In addition, an angular analysis of the decay products is presented, which provides the first measurement of the K^{*0} polarization fractions in this decay, giving $f_L = 0.50 \pm 0.08 \pm 0.02$, $f_{\parallel} = 0.19_{-0.08}^{+0.10} \pm 0.02$, and an S-wave contribution of $|A_S|^2 = 0.07_{-0.07}^{+0.15}$ in a $\pm 40 \text{ MeV}/c^2$ window around the K^{*0} mass.

We express our gratitude to our colleagues in the CERN accelerator departments for the excellent performance of the LHC. We thank the technical and administrative staff at CERN and at the LHCb institutes, and acknowledge support from the National Agencies: CAPES, CNPq, FAPERJ and FINEP (Brazil); CERN; NSFC (China); CNRS/IN2P3 (France); BMBF, DFG, HGF and MPG (Germany); SFI (Ireland); INFN (Italy); FOM and NWO (The Netherlands); SCSR (Poland); ANCS (Romania); MinES of Russia and Rosatom (Russia); MICINN, XuntaGal and GENCAT (Spain); SNSF and SER (Switzerland); NAS Ukraine (Ukraine); STFC (United Kingdom); NSF (USA). We also acknowledge the support received from the ERC under FP7 and the Region Auvergne.

References

- [1] S. Faller, R. Fleischer, and T. Mannel, *Precision physics with $B_s^0 \rightarrow J/\psi \phi$ at the LHC: the quest for new physics*, Phys. Rev. **D79** (2009) 014005, [arXiv:0810.4248](https://arxiv.org/abs/0810.4248).
- [2] CDF collaboration, T. Aaltonen *et al.*, *Observation of $B_s^0 \rightarrow J/\psi K^*(892)^0$ and $B_s^0 \rightarrow J/\psi K_S^0$ decays*, Phys. Rev. **D83** (2011) 052012, [arXiv:1102.1961](https://arxiv.org/abs/1102.1961).
- [3] Particle Data Group, K. Nakamura *et al.*, *Review of particle physics*, J. Phys. **G37** (2010) 075021.
- [4] Belle collaboration, K. Abe *et al.*, *Measurements of branching fractions and decay amplitudes in $B \rightarrow J/\psi K^*$ decays*, Phys. Lett. **B538** (2002) 11, [arXiv:hep-ex/0205021](https://arxiv.org/abs/hep-ex/0205021).
- [5] LHCb collaboration, A. A. Alves Jr. *et al.*, *The LHCb detector at the LHC*, JINST **3** (2008) S08005.
- [6] T. Sjöstrand, S. Mrenna, and P. Skands, *PYTHIA 6.4 Physics and manual*, JHEP **05** (2006) 026, [arXiv:hep-ph/0603175](https://arxiv.org/abs/hep-ph/0603175).
- [7] I. Belyaev *et al.*, *Handling of the generation of primary events in GAUSS, the LHCb simulation framework*, Nuclear Science Symposium Conference Record (NSS/MIC) IEEE (2010) 1155.

- [8] D. J. Lange, *The EvtGen particle decay simulation package*, Nucl. Instrum. Meth. **A462** (2001) 152.
- [9] P. Golonka and Z. Was, *PHOTOS Monte Carlo: a precision tool for QED corrections in Z and W decays*, Eur. Phys. J. **C45** (2006) 97, [arXiv:hep-ph/0506026](https://arxiv.org/abs/hep-ph/0506026).
- [10] GEANT4 collaboration, J. Allison *et al.*, *Geant4 developments and applications*, IEEE Trans. Nucl. Sci. **53** (2006) 270; GEANT4 collaboration, S. Agostinelli *et al.*, *GEANT4: a simulation toolkit*, Nucl. Instrum. Meth. **A506** (2003) 250.
- [11] M. Clemencic *et al.*, *The LHCb simulation application, Gauss: design, evolution and experience*, J. of Phys: Conf. Ser. **331** (2011) 032023.
- [12] D. Martínez Santos, *Study of the very rare decay $B_s \rightarrow \mu^+ \mu^-$ in LHCb*, PhD thesis, University of Santiago de Compostela, 2010, CERN-THESIS-2010-068.
- [13] D. Karlen, *Using projections and correlations to approximate probability distributions*, Comput. Phys. **12** (1998) 380, [arXiv:physics/9805018](https://arxiv.org/abs/physics/9805018).
- [14] BABAR collaboration, B. Aubert *et al.*, *Search for the $Z(4430)^-$ at BABAR*, Phys. Rev. **D79** (2009) 112001, [arXiv:0811.0564](https://arxiv.org/abs/0811.0564).
- [15] BABAR collaboration, B. Aubert *et al.*, *Time-integrated and time-dependent angular analyses of $B \rightarrow J/\psi K\pi$: a measurement of $\cos 2\beta$ with no sign ambiguity from strong phases*, Phys. Rev. **D71** (2005) 032005, [arXiv:hep-ex/0411016](https://arxiv.org/abs/hep-ex/0411016).
- [16] T. Skwarnicki, *A study of the radiative cascade transitions between the Upsilon-prime and Upsilon resonances*, PhD thesis, Institute of Nuclear Physics, Krakow, 1986, DESY-F31-86-02.
- [17] LHCb collaboration, R. Aaij *et al.*, *Measurement of b-hadron masses*, Phys. Lett. **B708** (2012) 241, [arXiv:1112.4896](https://arxiv.org/abs/1112.4896).
- [18] D0 collaboration, V. Abazov *et al.*, *Measurement of the angular and lifetime parameters of the decays $B_d^0 \rightarrow J/\psi K^{*0}$ and $B_s^0 \rightarrow J/\psi \phi$* , Phys. Rev. Lett. **102** (2009) 032001, [arXiv:0810.0037](https://arxiv.org/abs/0810.0037).
- [19] CDF collaboration, T. Aaltonen *et al.*, *Angular analysis of $B_s^0 \rightarrow J/\psi \phi$ and $B \rightarrow J/\psi K^*$ decays and measurement of $\Delta\Gamma_s$ and ϕ_s* , CDF public note (2011), CDF public note 8950.
- [20] T. du Pree, *Search for a strange phase in beautiful oscillations*, PhD thesis, Vrije Universiteit (Amsterdam), 2010, CERN-THESIS-2010-124.
- [21] LHCb collaboration, R. Aaij *et al.*, *Measurement of b hadron production fractions in 7 TeV pp collisions*, Phys. Rev. **D85** (2012) 032008, [arXiv:1111.2357](https://arxiv.org/abs/1111.2357).
- [22] K. De Bruyn *et al.*, *Branching ratio measurements of B_s decays*, Phys. Rev. **D86** (2012) 014027, [arXiv:1204.1735](https://arxiv.org/abs/1204.1735).